universe

MDPI

Article

The Barium Odd Isotope Fractions in Seven Ba Stars

Fang Wen [1], Wenyuan Cui [1,*], Miao Tian [1], Xiaoxiao Zhang [1], Jianrong Shi [2,3] and Bo Zhang [1]

[1] College of Physics, Hebei Normal University, Shijiazhuang 050024, China
[2] Key Lab of Astronomy, National Astronomical Observatories, Chinese Academy of Sciences, Beijing 100012, China
[3] School of Astronomy and Space Science, University of Chinese Academy of Sciences, Beijing 100049, China
* Correspondence: wenyuancui@126.com or cuiwenyuan@hebtu.edu.cn

Abstract: Based on the spectra with high resolution and a high signal-to-noise ratio, we investigate the enrichment history of the s-process element in seven barium (Ba) stars by measuring their Ba odd isotope fraction. It is found that the relative contributions of the s-process to their Ba abundance are $91.4 \pm 25.7\%$, $91.4 \pm 34.3\%$, $82.9 \pm 28.5\%$, $77.1 \pm 31.4\%$, and $71.4 \pm 37.1\%$ for REJ 0702+129, HD 13611, BD+80°670, HR 5692, and HD 202109, respectively. Our results suggest that these five Ba stars have a prominent s-process signature, which indicates that their heavy elements mainly come from their former AGB companions (now WDs) by mass transfer, while the r-process contribution can naturally be explained by the evolution of the Milky Way. The s-process contribution of BD+80°670 is $51.4 \pm 31.4\%$, which is the lowest among our seven sample stars. Considering its lower values of both [Ba/Nd] and [Ba/Eu], we suspect that BD+68°1027 is likely to be a r-rich Ba star and has similar origins to the CEMP-r/s stars. HD 218356 has an unreasonable s-process contribution over 100%. Combining its stellar atmospheric parameters and the evolutionary stage, we speculate that HD 218356 is a more evolved extrinsic Ba star, and its massive companion should have the largest s-process efficiency in our samples.

Keywords: stars; abundance of binaries; general stars; chemically peculiar stars; AGB; post-AGB

check for updates

Citation: Wen, F.; Cui, W.; Tian, M.; Zhang, X.; Shi, J.; Zhang, B. The Barium Odd Isotope Fractions in Seven Ba Stars. *Universe* **2022**, *8*, 596. https://doi.org/10.3390/universe8110596

Academic Editor: Sylvia Ekström

Received: 13 October 2022
Accepted: 9 November 2022
Published: 12 November 2022

1. Introduction

Barium stars can be divided into Ba dwarfs and Ba giants according to their evolution stage, which is characterized by the enrichment of heavy elements such as Ba, La, Ce, etc. Ba giants, usually of the spectral type G and K, were first observed by Bidelman and Keenan [1], while the dwarf HR 107 with the spectral type F5V, which shows the mild overabundance of s-process elements, was first classified as a Ba dwarf star by Tomkin et al. [2].

In the solar system, 85% of barium is produced by the s-process [3], which is expected to take place in low-mass stars ($M < 3.0\,M_{\odot}$ [4,5]) during their asymptotic giant branch (AGB) phase. The rest are from the r-process [3], which usually arises with explosive events such as core-collapse supernovae (SNe II, $M > 8\,M_{\odot}$, [6]) and neutron star mergers [7,8]. It is found that all of the Ba dwarfs and most of the Ba giants are not able to produce s-process elements by themselves due to their lower luminosity than AGB stars. The enriched heavy elements in these Ba stars were suggested to come from an AGB companion (now a white dwarf (WD)) by mass transfer [9]. Such kinds of Ba stars are defined as extrinsic Ba stars, and their companions have also been confirmed through the radial velocity monitoring of most of them [10–13]. On the contrary, the intrinsic Ba stars are those having reached the AGB stage and brought the newly produced Ba from the nucleosynthesis region to the surface by the third dredge-up mechanism.

Due to the longer cooling timescale of WD companions compared to the lifetime of Ba stars on their giant branch, Böhm-Vitense et al. [11] suggested that the mass transfer of Ba-rich material might happen when their sample Ba giants are still in the main sequence. This means that Ba giants may have evolved from Ba dwarfs; in such a case, more Ba

dwarfs should be expected. In fact, since the first Ba dwarf HR 107 was observed, more Ba dwarfs with spectral types of F to G have been identified successively [14–21]; however, the number of known Ba dwarfs to date is still considerably smaller than that of Ba giants. North and Lanz [22] did not find any UV excess related to the presence of the expected WD companions of their three Ba dwarfs, and the existence of WD companions for the five Ba dwarfs identified by Edvardsson et al. [23] was also not confirmed through a long-term radial velocity monitoring (for details, see [24]). This means that the origin of Ba dwarfs, at least for some of them, and the correlation between Ba giants and dwarfs should be further studied.

The ratio of s- and r-process contributions to heavy elements in Ba dwarfs and giants could shed light on their origin histories, and the s- and r-process signatures can be detected directly in a star by measuring the fraction of Ba odd isotopes ($f_{\mathrm{odd,Ba}}$)[1] from the Ba II resonance line (4554 Å) profile. This method was first adopted by Cowley and Frey [25] and Magain and Zhao [26]. According to Arlandini et al. [27], the $f_{\mathrm{odd,Ba}}$ value is 0.11 for a pure s-process origin, while 0.46 for a pure r-process. The in between values of $f_{\mathrm{odd,Ba}}$ represent a mixed contribution, and a higher $f_{\mathrm{odd,Ba}}$ value means a larger contribution from the r-process. To investigate the contribution of the r-process, measurements of $f_{\mathrm{odd,Ba}}$ have been conducted for the metal-poor star HD 140283 in a series of literature works [28–32], for the thin and thick disk stars of the Milky Way [33], and for the CEMP-r/s star HE 0338-3945 and five r-II stars,CS 31082-001, CS 29491-069, HE 1219-0312, HE 2327-5642, and HE 2252-4225 [34,35].

In order to study the contributions of the r- and s-process to barium and other heavy elements ($Z > 30$), in this paper, we measured the $f_{\mathrm{odd,Ba}}$ values for three Ba dwarfs and four Ba giants, which will help us better understand their origins. In Section 2, the observations and data reduction are presented. The determination of the stellar atmospheric parameters of our sample stars is described in Section 3, while the measurement of the Ba abundance and Ba isotope fractions is presented in Section 4. Our results are shown in Section 5, and the conclusions are given in Section 6.

2. Observations and Data Reduction

Our sample includes three Ba dwarfs and four Ba giants, and the basic data collected from Holberg et al. [36] and Kong et al. [24,37] are listed in Table 1. All of these stars belong to the group of the so-called "Sirius-like system", which is a binary or a multi-star system. The Sirius-like system contains a known WD and at least one component of spectral type K or earlier [36].

Table 1. Basic data of the seven barium stars.

Star	Type	V_{mag}	a (au)	ϖ (mas)	Spectrograph	Remark
BD+80°670	G5V	9.16	833.8	15.48 ± 0.15	ARCES	dwarf
BD+68°1027	G5	9.46	3027.8	11.43 ± 0.01	ARCES	dwarf
REJ 0702+129	K0IV/V	10.53	–	8.35 ± 0.48	ARCES	dwarf
HD 218356	K1IV	4.91	–	5.18 ± 0.11	CES	giant
HD 202109	$G8III_p$	3.31	1.8	21.81 ± 0.14	CES	giant
HR 5692	G8II-III	5.80	2.0	7.79 ± 0.22	CES	giant
HD 13611	G6II/III	4.47	3.8	10.42 ± 0.35	CES	giant

The high-resolution and high-signal-to-noise (S/N) spectra were taken from Xiaoming Kong (2020 private communication). The spectra of three Ba dwarfs were observed with the ARC Echelle Spectrograph (ARCES) mounted on the 3.5 m telescope at the Apache Point Observatory (APO), during the nights of 23 October and 11 November 2014, and they have a resolution power of R∼31,500 with a wavelength range of 4400–10,000 Å. The spectra of four Ba giants were observed with the echelle spectrograph (CES) mounted on the 2.16 m telescope located at Xinglong station, China, during March and September 2015, and cover

a wavelength range from 4000 to 9000 Å with a resolution power of R∼50,000 (for details, see [37]). The signal-to-noise ratios (S/Ns) of all spectra are higher than 100.

3. Stellar Parameters and Model Atmospheres

The stellar atmospheric parameters of our sample Ba stars were determined by Kong et al. [24,37], and they used the 1D MARCS-OS model atmospheres (see [38]), assuming local thermal equilibrium (LTE) when deriving the iron abundances. It was noted by Asplund [39] and Sitnova et al. [40] that the non-local thermal equilibrium (NLTE) effects of Fe lines are important, and they need to be considered for giants especially.

In order to reduce the uncertainties of the final results, we redetermined the stellar atmospheric parameters of seven sample stars including the NLTE effects of the iron lines. The MAFAGS opacity sampling (OS) model, which was developed by Grupp [41] and updated by Grupp et al. [42], was applied in the analysis, and the atomic data computed by Kurucz [43–45] were incorporated in the new version. We performed the line formation using the IDL/Fortran SIU software package of Reetz [46]. The effective temperature ($T_{\rm eff}$) was obtained by requiring the same iron abundance derived from Fe I lines with different excitation potentials (EPs), and the surface gravity ($\log g$) was determined through the Fe I and Fe II ionization equilibrium method, i.e., requiring the same iron abundances from the Fe I and Fe II lines. The microturbulence velocity (ξ) was derived when the iron abundances were independent of their equivalent widths (EWs). Around 25 Fe I lines with moderate intensity were adopted, which were selected from Mashonkina et al. [47] and Bensby et al. [48]. The iron abundances were measured through the spectral synthesis method, and the NLTE effects were considered. In our study, the model atom of Fe I was constructed using the levels with E_{exc} up to 7.897 eV including in total 2970 levels, and the coupled radiative transfer and SE equations were solved with a revised version of the DETAIL code (Butler and Giddings [49]). As an example, the abundances from the Fe I and Fe II lines of two stars BD+80°670 and HR 5692 versus EPs and EWs are shown in Figure 1. The final stellar atmospheric parameters are shown in Table 2, and the results from Kong et al. [24,37] are also included for comparison.

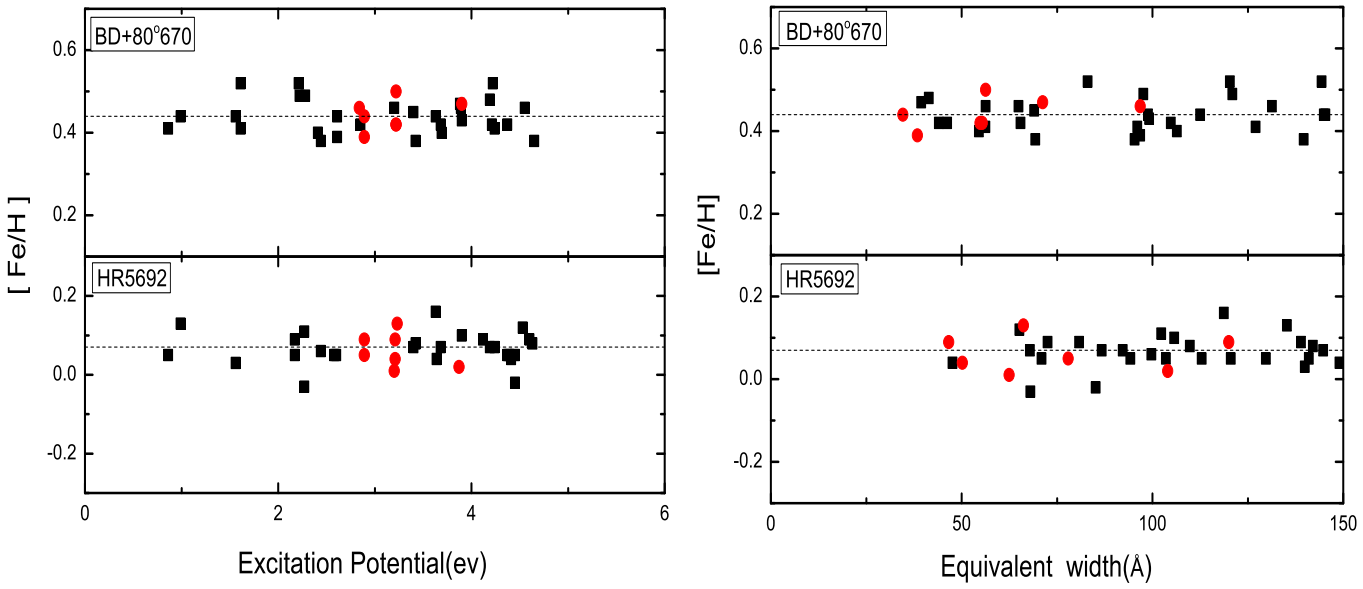

Figure 1. The iron abundances of our sample stars from Fe I_{NLTE} (filled triangles) and Fe II_{LTE} (filled circles) versus excitation potentials (**left**) and equivalent widths (**right**).

We compared the effective temperatures determined by us with those of [24,37] for the sample stars in Figure 2, and a consistent result can be found. The largest difference in temperature was for the giant star HD 218356; however, it was still around 100 K.

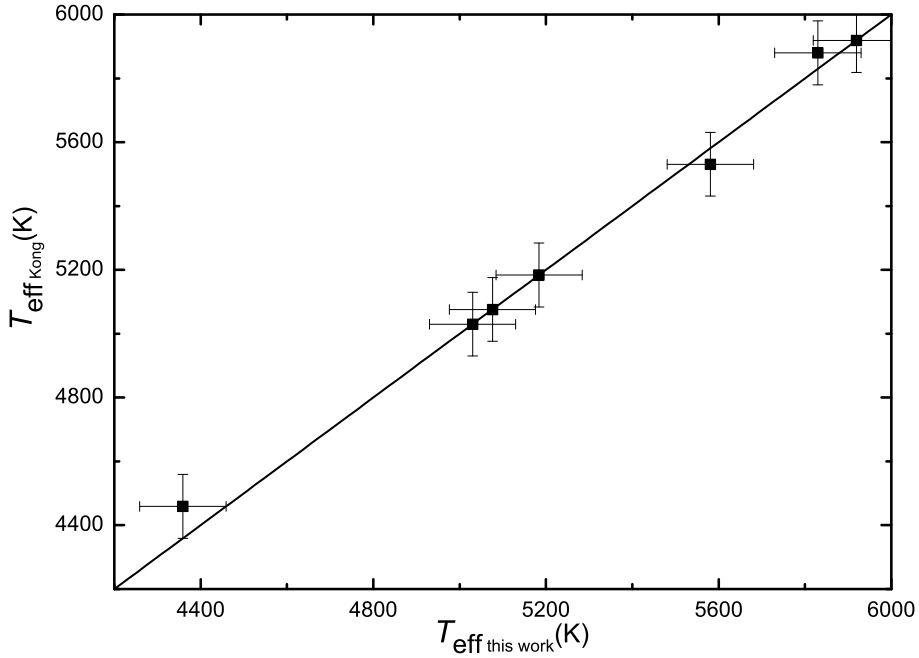

Figure 2. The comparison of the effective temperatures determined in this work with those of Kong et al. [24,37] for the sample stars.

We also calculated the surface gravities ($\log g$) based on the parallax from *Gaia* DR3 [50,51] using the relation:

$$\begin{aligned} \log\, g &= \log\, g_{\odot} + \log\,(\frac{M}{M_{\odot}}) + 4\log\,(\frac{T_{\rm eff}}{T_{\rm eff\odot}}) + 0.4(M_{\rm bol} - M_{\rm bol\odot}), \\ M_{\rm bol} &= V_{\rm mag} + BC + 5\log\,\varpi + 5 - A_{\rm V}. \end{aligned} \tag{1}$$

where M is the stellar mass, which can be estimated based on the theoretical isochrones with a Bayesian estimation method [52]. BC is the bolometric correction and can be calculated from the relation given by Alonso et al. [53]. $V_{\rm mag}$ is the apparent magnitude and was obtained from the UCAC4 catalog. We adopted the parallax ϖ from *Gaia* DR3 [50,51]. $A_{\rm V}$ represents the interstellar extinction, which was calculated based on Schlegel et al. [54] and Beers et al. [55]. The results are given in Table 2, and for comparison, the $\log g$ values from Kong et al. [24,37] are also included. The comparison of the $\log g$ values derived from both methods in this work is shown in Figure 3, and a consistent result with a difference of 0.08 ± 0.04 dex can be found.

We obtained the masses of the sample stars (in Table 2) from the website (http://stev.oapd.inaf.it/cgi-bin/param_1.3) (accessed on 12 October 2021), which performs the Bayesian estimation of stellar parameters. The stellar masses are related to the effective temperature, metal abundance, apparent magnitude, and parallax. We set their errors to be 100K, 0.06 dex, and 0.05 dex, respectively, and the errors of the parallax are shown in Table 1. Then, we determined the mass error of HD 218356 to be $\pm 0.38\ M_{\odot}$, while the mass errors of the other six stars were all less than $\pm 0.11\ M_{\odot}$.

The uncertainty of atmospheric parameters arises mainly from the errors of the iron abundances from the Fe I and Fe II lines and equivalent widths of the Fe I lines. When $\log g$ is calculated using Equation (1), its error is also related to parameters such as the apparent magnitude and parallax. The final uncertainties in $T_{\rm eff}$, $\log g$, [Fe/H], and ξ were estimated to be ± 100 K, ± 0.1 dex, ± 0.06 dex, and ± 0.15 km s^{-1}, respectively.

Table 2. The stellar atmospheric parameters and masses of our sample stars.

Star	$T_{\rm eff}$ (K)	log g (Spec)	log g (Parallax)	ξ (km s^{-1})	[Fe/H] (NLTE)	[Fe/H] (LTE)	M ($M_{\odot}$)	References [a]
BD+80°670	5830	4.50	4.45	1.00	0.44	0.41	1.09	This work
	5880	4.50	4.33	1.60	-	0.13	1.05	KONG18(a)
BD+68°1027	5919	4.55	4.39	1.00	−0.35	−0.36	0.91	This work
	5919	4.55	4.48	1.00	-	−0.31	0.93	KONG18(a)
REJ 0702+129	5581	4.50	4.45	1.50	0.13	0.11	0.98	This work
	5531	4.20	-	1.90	-	−0.06	0.93	KONG18(a)
HD 218356	4359	1.50	1.41	2.20	−0.58	−0.59	2.03	This work
	4459	1.87	1.67	1.90	-	−0.43	2.50	KONG18(b)
HD 202109	5030	2.70	2.61	1.90	−0.13	−0.15	2.66	This work
	5010	2.70	2.68	1.70	-	−0.01	3.20	KONG18(b)
HR 5692	5076	2.83	2.70	1.30	0.07	0.05	2.63	This work
	5076	2.83	2.86	1.30	-	0.02	2.80	KONG18(b)
HD 13611	5184	2.60	2.36	1.50	−0.02	−0.02	3.20	This work
	5184	2.60	2.45	1.50	-	−0.01	3.80	KONG18(b)

a: KONG18(a): Kong et al. [24], KONG18(b): Kong et al. [37].

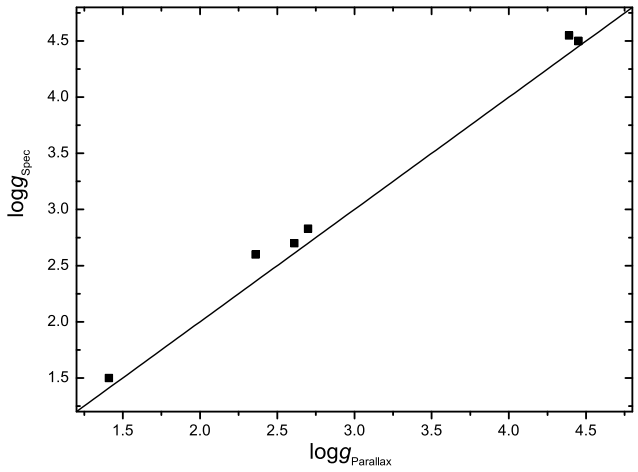

Figure 3. The comparison of the surface gravity derived by the parallaxes of Gaia DR3 with those from the spectra method in this work.

4. The Barium Odd Isotopic Fractions

4.1. Ba Abundance

We employed the Ba II subordinate lines at 5853 and 6496 Å to determine the Ba abundance of our sample stars, which suffer small hyper-fine splitting (HFS) effects. In order to obtain more accurate results, the NLTE effect was considered in the measurement of Ba abundance, and the atomic model was adopted from Mashonkina et al. [56]. The Ba atomic model includes the energy levels with $n \leqslant 12$ and $l \leqslant 4$, and the fine structure of the $5d^2D$ and $6p^2P^0$ terms were considered. The nf and $(n-1)$g levels were combined due to the small excitation energy differences between them. Therefore, there were 35 bound levels of Ba II and the ground state of Ba III. The final Ba abundance is the average of the two lines above, and the final Ba abundance of our sample stars with and without NLTE effects considered is shown in Table 3. For HR 5692 and HD 13611, we could not obtain their Ba abundance from the Ba II line at 6496 Å, as the S/N of the spectrum at this wavelength region is low. It can be found that the NLTE effects of the two subordinate lines were no more than 0.08 dex for our sample stars, as shown in Table 3.

We note that our LTE Ba abundances of BD+68°1027, HD 5692, and HD 13611 were consistent with those of Kong et al. [24,37] within the errors. The Δ[Ba/Fe]$_{\rm LTE}$ for BD+80°670, REJ 0702+129 were 0.19 and 0.12 dex, which was mainly due to the differences of the microturbulence velocities and [Fe/H] obtained by this work and the literature, that is

$\Delta\xi = 0.6, 0.4$ and $\Delta[\mathrm{Fe/H}] = 0.28, 0.21$, respectively. For HD 218356, $\Delta[\mathrm{Ba/Fe}]_{\mathrm{LTE}}$ is mainly brought by ΔT_{eff} = 100 K, $\Delta \log g = 0.37$, and $\Delta\xi = 0.3$. The lower metallicity adopted by us was the dominant reason for the $\Delta[\mathrm{Ba/Fe}]_{\mathrm{LTE}} = 0.13$ dex of HD 202109.

Table 3. The Ba abundances of our seven stars with NLTE and LTE considered.

Star	5853.67Å		6496.90Å		[Ba/Fe] [a]		[Ba/Fe] [b]	$f_{\mathrm{odd,Ba}}$	Contribution (%)
	LTE	NLTE	LTE	NLTE	LTE	NLTE	LTE	s-Process	
BD+80°670	0.48	0.46	0.53	0.48	0.50 ± 0.04	0.47 ± 0.01	0.31 ± 0.03	0.17 ± 0.10	82.86
BD+68°1027	0.67	0.62	0.72	0.64	0.70 ± 0.04	0.63 ± 0.01	0.62 ± 0.07	0.28 ± 0.11	51.43
REJ 0702+129	0.67	0.63	0.70	0.68	0.68 ± 0.04	0.65 ± 0.04	0.56 ± 0.06	0.14 ± 0.09	91.43
HD 218356	1.10	1.02	1.14	1.06	1.12 ± 0.03	1.04 ± 0.03	1.01 ± 0.11	0.08 ± 0.10	100.00
HD 202109	0.60	0.56	0.70	0.67	0.65 ± 0.07	0.62 ± 0.08	0.52 ± 0.14	0.21 ± 0.13	71.43
HD 5692	0.64	0.60	-	-	0.64 ± 0.10	0.60 ± 0.10	0.61 ± 0.12	0.19 ± 0.11	77.14
HD 13611	0.54	0.50	-	-	0.54 ± 0.10	0.50 ± 0.10	0.52 ± 0.15	0.14 ± 0.12	91.43

[a]: this work; [b]: Kong et al. [24,37].

4.2. The Barium Odd Isotopic Fraction

The fractions of the s- and r- processes' contribution to the stellar heavy elements in the sample stars can illustrate their origins. The relative contributions of the s- and r-processes to heavy elements in a star can be estimated from the $f_{\mathrm{odd,Ba}}$ value. The reason is that, in the five stable Ba isotopes ^{134}Ba, ^{135}Ba,^{136}Ba, ^{137}Ba, and ^{138}Ba, there are two s-only nuclei, i.e., ^{134}Ba and ^{136}Ba. These two s-only nuclei are formed only by the s-process due to the shielding by ^{134}Xe and ^{136}Xe on the r-process path. Usually, a larger $f_{\mathrm{odd,Ba}}$ value corresponds to a higher r-process contribution.

In order to study the origin of the heavy elements in our sample stars, it is interesting to determine their $f_{\mathrm{odd,Ba}}$ values. For the strong Ba II resonance line at 4554 Å, the even isotopes are responsible for the line core, while the line wings are mainly influenced by the odd isotopes [31]. The strong HFS effect suffered by the odd isotopes results in an asymmetry in the line wings. Following the approach adopted by Mashonkina and Zhao [33], we first determined the Ba abundance of the sample stars (see Table 3), then the $f_{\mathrm{odd,Ba}}$ values were measured through fitting the line profile of Ba II 4554 Å with the above Ba abundance. The synthetic line profiles were computed using the IDL/Fortran SIU software package developed by Reetz [46], and the NLTE effect was considered during the line fitting.

In order to obtain the best-fitting results, a reduced χ^2 was applied, which is defined as:

$$\chi_r^2 = \frac{1}{\nu - 1} \sum_{i=1} \frac{(O_i - S_i)^2}{\sigma_i^2} \quad (2)$$

where O_i and S_i are the flux of the observed and synthetic normalized spectra at point i, respectively. ν is the number of the degrees of freedom in the fitting. σ_i is the standard deviation of the observed spectrum [57], which is defined as $\sigma_i = [(S/N)(f_i)^{1/2}]^{-1}$, where S/N is measured in a roughly 1 Å interval on either side of the referenced spectral line, and f_i indicates the normalized flux at the ith point ($0 \leq f_i \leq 1$ for absorption profiles) [58]. During the fitting, the total degrees of freedom ν were 21, 20, 23, 49, 46, 45, and 42 for BD+80°670, BD+68°1027, REJ 0702+129, HD 218356, HD 202109, HR 5692, and HD 13611, respectively.

In the process of measurement, we fixed the Ba abundances from Section 4.1 and varied the Ba odd isotope fraction $f_{\mathrm{odd,Ba}}$ freely until a minimum value of χ_r^2 was obtained. It is expected that the minimum χ_r^2 corresponds to the best fitting of the observed line profiles. The best fits to the Ba II line at λ4554 Å are presented in Figure 4, and the residuals (synthetic profile minus observed profile) are also included in the left panel from top to bottom for our sample stars, respectively. In the right panel of Figure 4, we show χ_r^2 versus $f_{\mathrm{odd,Ba}}$. The final values of $f_{\mathrm{odd,Ba}}$ are listed in Table 3.

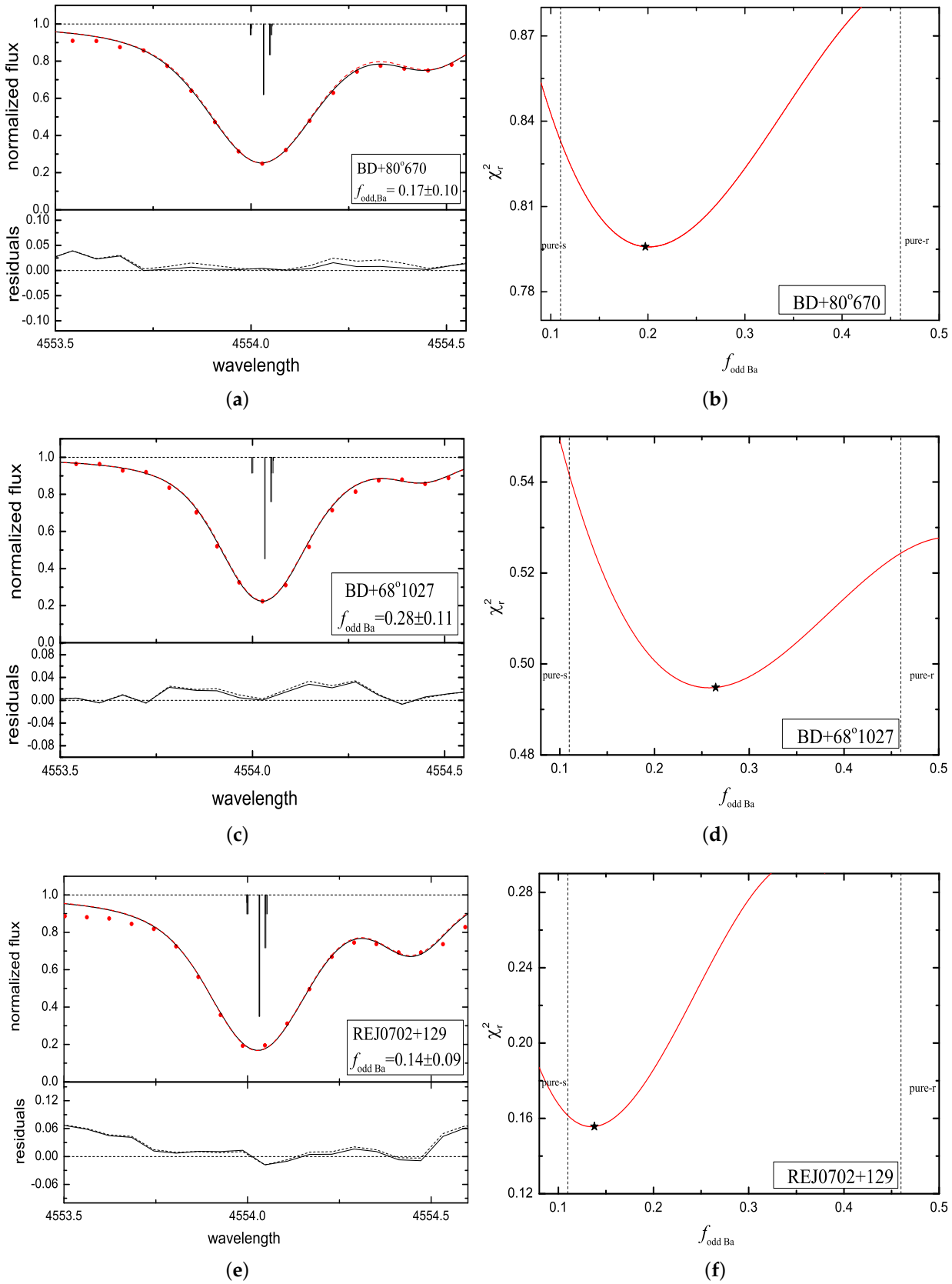

Figure 4. *Cont.*

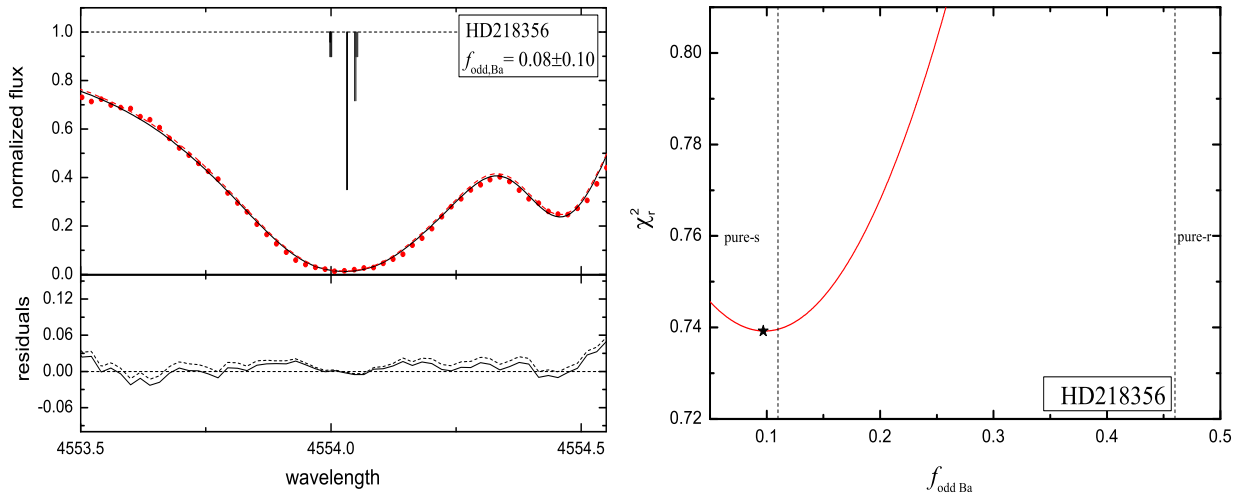

(**g**) (**h**)

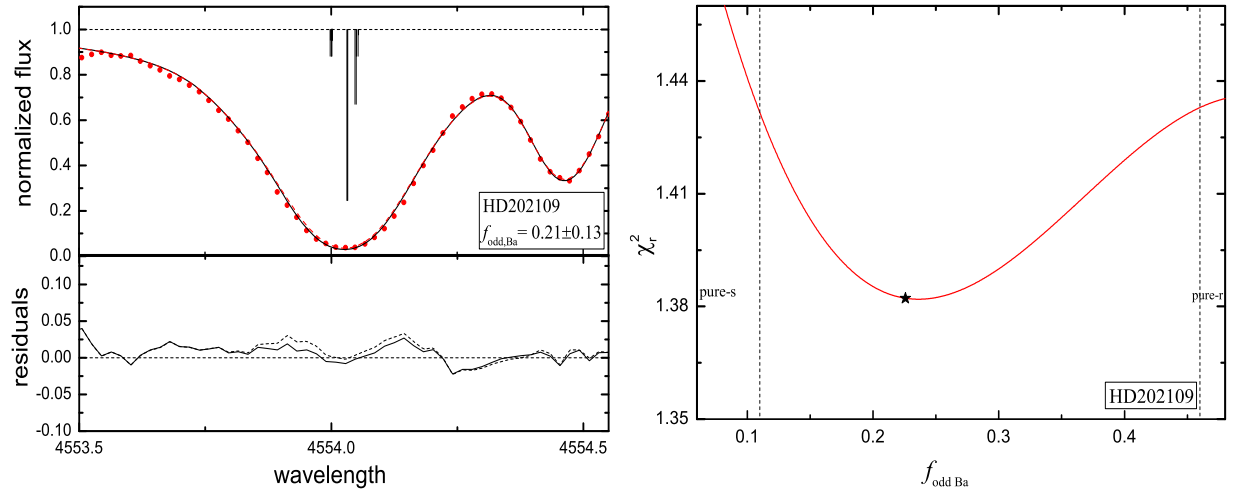

(**i**) (**j**)

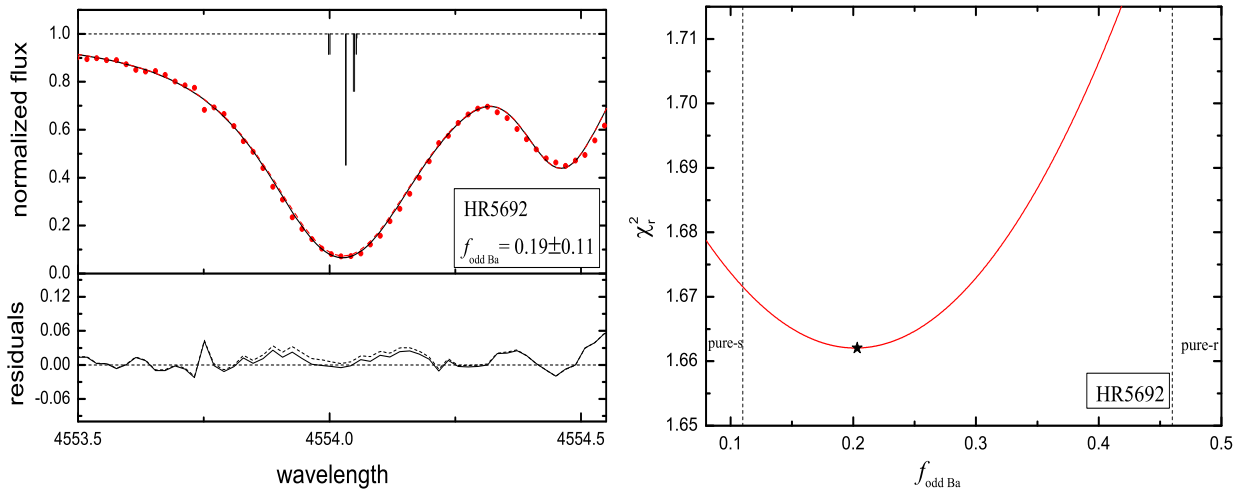

(**k**) (**l**)

Figure 4. *Cont.*

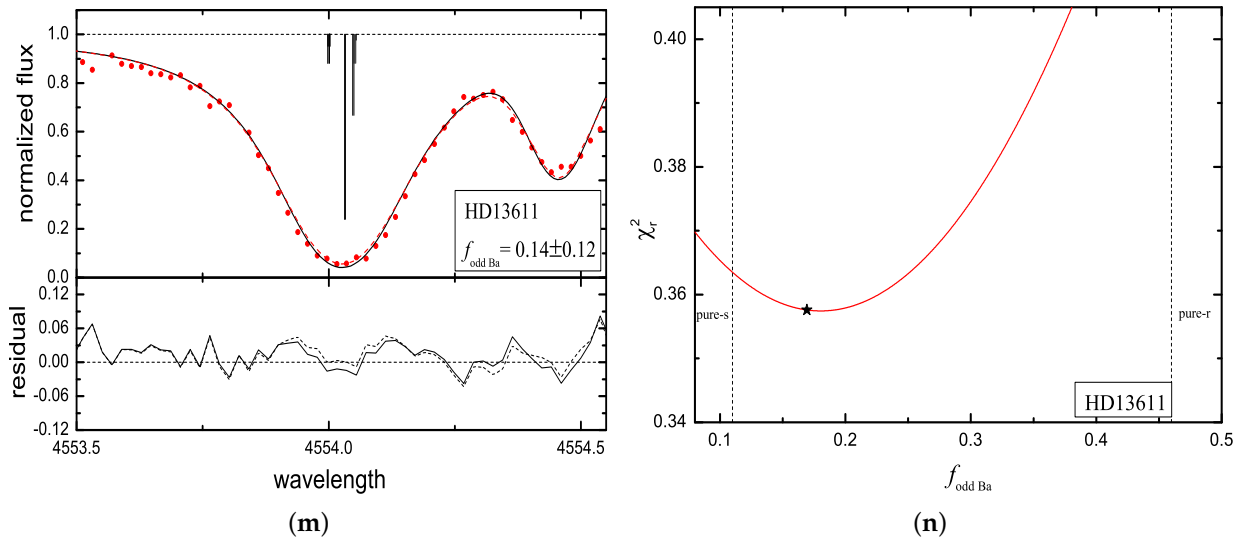

Figure 4. Left panel (**from top to bottom**): The best statistical fits of the synthetic profile to the observed (filled circles) Ba II resonance lines at 4554 Å for our sample Ba stars are shown in the sub-figure above, respectively. The residual plots of each sub-figure are shown below, respectively. The synthetic lines with $f_{\text{odd,Ba}} - \delta$ and the corresponding residuals are plotted (dotted lines) in each of the sub-figures for comparison. Right panel (**from top to bottom**): We show the χ^2 fit for the λ4554 line, and every black asterisk shows where the minimum of the fit lies. The vertical dotted lines indicate the $f_{\text{odd,Ba}}$ of the solar pure s-process (**left**) and pure r-process (**right**), respectively.

In Figure 4, we find that all except two stars (HD202109 and HR5692) have a χ^2_r value less than one in our sample stars. Based on the equations of χ^2_r and σ_i, the χ^2_r value is related to the S/N ratio at the line of Ba II 4554 Å. Aoki et al. [58] suggested that a larger S/N ratio can result in a χ^2_r value less than one. For five of our sample Ba stars, the smaller χ^2_r values were also due to the larger S/N ratios at the line 4554 Å.

Our synthetic spectra were calculated by convolving the macroturbulence (V_{mac}), the instrumental broadening value (Γ), and the rotational velocity ($v\sin i$) together. The square of the convolution value is equal to the sum of the squares of the three parameters above ($G = \sqrt{\Gamma^2 + V^2_{mac} + (v\,sin\,i)^2}$). The instrumental broadening value can be determined by a Gaussian fit to the Th-Ar lamp spectra corresponding to the studied Ba stars. We usually discuss the effect of macroturbulence on the $f_{\text{odd,Ba}}$ value, and here, we used the uncertainties of G to investigate the effects of the above factors on the Ba odd isotope fraction; the detailed results are shown in Table 4.

Table 4. The effect on the values of $f_{\text{odd,Ba}}$ due to the uncertainties of atomic data and stellar parameters.

Input Parameter	Input Error	BD +80°670	BD +68°1027	REJ 0702+129	HD 218356	HD 202109	HR 5692	HD 13611
T_{eff}	+100	+0.04	−0.02	+0.02	+0.02	−0.05	+0.02	−0.04
log g	−0.10	−0.02	+0.02	−0.01	+0.02	−0.01	+0.03	+0.03
ξ	+0.15	+0.03	+0.05	+0.06	+0.04	+0.07	+0.04	+0.04
$[Fe/H]$	−0.06	+0.03	+0.01	+0.01	−0.01	−0.01	−0.03	+0.02
log C_6(4554)	+0.10	−0.01	+0.02	−0.01	−0.03	+0.02	−0.03	−0.02
log gf(4554)	−0.10	+0.05	+0.06	+0.03	+0.05	+0.07	+0.06	+0.08
log $C_6(5d-6p)$	+0.10	−0.03	+0.01	+0.02	−0.05	−0.02	+0.02	−0.03
G	−0.20	+0.05	−0.06	−0.05	+0.04	−0.05	+0.06	−0.04
Ba abundance	+0.05	+0.03	−0.02	+0.01	+0.02	−0.03	−0.02	+0.01
$\Delta(total)$		±0.10	±0.11	±0.09	±0.10	±0.13	±0.11	±0.12

5. Origins of the Heavy Elements for Our Sample Barium Stars

According to Arlandini et al. [27], we know that $f_{\mathrm{odd,Ba}}$ = 0.46 corresponds to the pure r-process, while $f_{\mathrm{odd,Ba}}$ = 0.11 for the pure s-process. The solar value of $f_{\mathrm{odd,Ba}}$ is 0.18, which means that about 80% of the barium in the solar system is from the s-process, while about 20% from the r-process. This was calculated from the formula: s-process(%) = $[100-(f_{\mathrm{odd,Ba}} - 0.11)/0.0035]$ (see [31,34,35]). The relative contributions of the r- and s-processes to Ba in our sample stars were also calculated using the above formula, and the results are presented in Table 3.

5.1. AGB Model Predictions

The s-process nucleosynthesis usually occurs in the AGB stars, and we present the theoretical Ba odd isotope fractions calculated from the FRANEC Repository of Updated Isotopic Tables & Yields (FRUITY) database (http://www.oa-teramo.inaf.it/fruity) (accessed on 12 January 2022) as a function of [Fe/H] in Figure 5. Only the AGB model results with a mass range from 1.3 to 4.0 $M_{\odot}$ are presented. For convenience, the model results with the standard ^{13}C-pocket and 0 km/s of the initial rotational velocity were adopted [59].

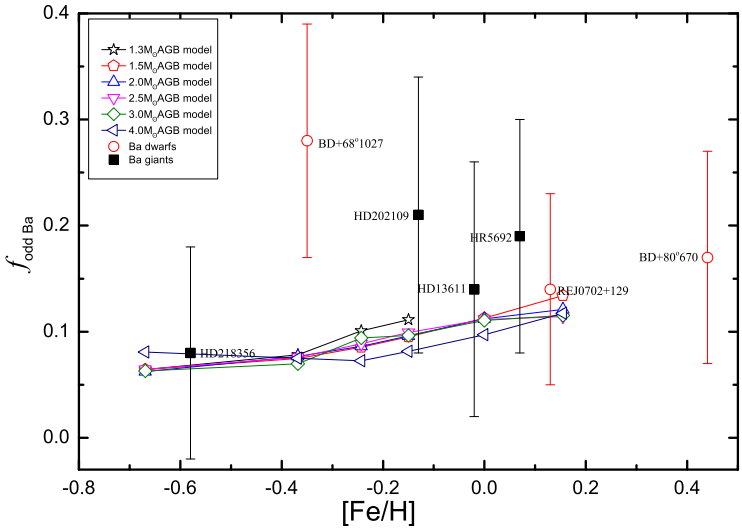

Figure 5. The Ba odd isotope fractions predicted by the AGB model versus [Fe/H] based on the FRANEC Repository of Updated Isotopic Tables & Yields (FRUITY) database, which provides the nucleosynthesis of AGB stars with different masses: 1.3, 1.5, 2.0, 2.5, 3.0, and 4.0 $M_{\odot}$, and with no initial rotation [59]. Our sample stars are also presented in the figure.

As shown in Figure 5, we found that the values of $f_{\mathrm{odd,Ba}}$ decrease from about 0.12 to 0.06 when [Fe/H] decreases from +0.16 to −0.7 dex, which is different from the solar pure s-process value of 0.11. The reason is that the contribution of the solar pure s-process is the superposition result of the contributions of multi-generation AGB stars. The decreasing trend of $f_{\mathrm{odd,Ba}}$ with decreasing [Fe/H] can be explained by the fact that the s-process produces heavy elements, such as Ba, Pb, etc., more efficiently under metal-poor conditions because of the primary nature of the ^{13}C neutron source [4]. ^{13}C(α,n)^{16}O is the major neutron source of the s-process nucleosynthesis in AGB stars, where the production of ^{13}C is independent of [Fe/H]. This means the neutron density is also independent of [Fe/H] in the s-process region; thus, the number ratio of neutron-to-iron-seed is higher at low metallicities, which is more conducive to the production of heavier elements [60]. In addition, the reduction of neutron poisons such as ^{16}O, ^{22}Ne, and ^{25}Mg, etc., under metal-poor conditions is also conducive to produce heavy elements.

5.2. Origin of the Five Normal Ba Stars

The two Ba dwarfs BD+80°670 and REJ 0702+129 and three Ba giants HD 13611, HR 5692, and HD 202109 have $f_{\mathrm{odd,Ba}}$ values around 0.14−0.21 (see Table 3), and they are

similar to that of the solar (0.18), which corresponds to an s-process contribution of about 91–71%. In general, the s-process is usually expected to occur in AGB stars, but the five Ba stars have not yet evolved to the AGB stage based on their $\log g$ values. McClure et al. [9] proposed a mass transfer scenario in a binary system to explain the enriched heavy elements of Ba stars, that is to say, the massive companion (now WD) firstly evolves to the AGB phase and produces heavy elements, then transfers them to the Ba stars by wind.

We plot the $f_{\mathrm{odd,Ba}}$ values of the five Ba stars in Figure 5 for comparison, and it can be seen that their $f_{\mathrm{odd,Ba}}$ values are slightly higher than those of the AGB models, which means that the AGB models alone could not explain their Ba abundances. As noted by Kong et al. [24,37], all of our five Ba stars have WD companions. Thus, we deduced that that the enriched barium of the five Ba stars has a dominant s-process origin, and their r-process contributions come from the interstellar medium, similar to our Sun, and is the pollution result of a long-term r-process event in the Milky Way.

5.3. An Intrinsic Ba Star HD 218356?

The Ba giant HD 218356 has a $f_{\mathrm{odd,Ba}}$ value of 0.08, corresponding to an s-process contribution over 100%, which is unreasonable. The reason is that in the formula: s-process(%) = $[100-(f_{\mathrm{odd,Ba}}-0.11)/0.0035]$, we adopted the solar $f_{\mathrm{odd,Ba}}$ value of 0.11 as the pure s-process standard value, which is the result of the chemical evolution of the Milky Way. The metallicity of HD 218356 is -0.58 dex, which is much lower than the solar one. It can be found from Figure 5 that all of the AGB models of [Fe/H] < -0.2 dex with different initial masses result in lower $f_{\mathrm{odd,Ba}}$ values, which indicates a higher s-process nucleosynthesis efficiency in the environment with the lower metallicity. As a result, the standard value of $f_{\mathrm{odd,Ba}}$ for the pure s-process in the stellar medium at [Fe/H] $= -0.58$ dex is likely to be lower than the solar one (0.11).

The $f_{\mathrm{odd,Ba}}$ value of HD 218356 is consistent with the results of the AGB model with $4\,M_{\odot}$ of [Fe/H] $= -0.58$ dex, as shown in Figure 5; however, the AGB models with other masses, i.e., 1.3, 1.5, 2.0, 2.5, $3.0\,M_{\odot}$, can still not be ruled out considering the error of the $f_{\mathrm{odd,Ba}}$. The mass of HD 218356 obtained here is around $2.03\,M_{\odot}$ (see Table 2), which was based on its stellar atmospheric parameters. Both the s-process contribution and comparison with the AGB models support that the barium in HD 218356 is dominated by the s-process. In other words, it should be an intrinsic Ba star, and all of its barium is likely to be produced by the s-process. Moreover, both Kong et al. [37] and Bubar and King [61] reported that HD 218356 shows overabundance of Na, i.e., [Na/Fe] = 0.33 and 0.53 dex, respectively, whereas the other Ba stars in our sample have normal Na abundances. Williams et al. [62] noted that a large amount of Na could be produced in the interiors of AGB stars and then brought up to their surface.

In Figure 6, the evolution track from the subgiant branch (SGB) to post-AGB is presented, which was calculated for a star with $2.1\,M_{\odot}$ and [Fe/H] $= -0.58$ dex using the MIST model [63–67]. As there are no data on the website (http://waps.cfa.harvard.edu/MIST/) (accessed on 12 January 2022). If copyright is needed for a star with $2.03\,M_{\odot}$ and [Fe/H] $= -0.58$ dex, we adopted the $2.1\,M_{\odot}$ model results instead. The theoretical results of the $\log g$ values range from around -0.72 to 2.35 dex between the EAGB and TP-AGB, and those of $\log T_{\mathrm{eff}}$ were from 3.47 to 3.69. From Figure 6, we can see that HD 218356 is likely to be in the early AGB (EAGB) stage, and it is before the thermally pulsating AGB (TP-AGB) phase based on its $\log g = 1.50$ dex and $\log T_{\mathrm{eff}} = 3.64$. This means that neither s-process nucleosynthesis nor the so-called third dredge-up event occur in this star.

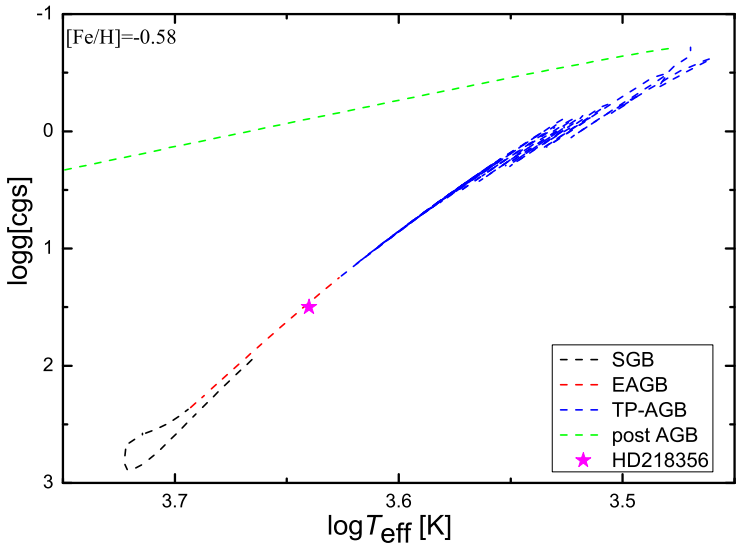

Figure 6. The stellar evolutionary track of a star with 2.1 $M_{\odot}$ and [Fe/H] = −0.58 dex calculated using the MIST model. The evolution phases from the SGB to post-AGB are presented. The filled red asterisk represents the Ba giant HD 218356.

In conclusion, we inferred that HD 218356 should still belong to the group of extrinsic Ba stars, and its massive companion should have the largest s-process efficiency considering its largest NLTE Ba abundance of [Ba/Fe] = 1.04 dex and the lowest value of $f_{\mathrm{odd,Ba}} = 0.08 \pm 0.10$ in our Ba samples.

5.4. An r-Rich Ba Star, BD+68°1027

It is known that some of the carbon-enhanced metal-poor stars are enriched with both the r- and s-process elements (CEMP-r/s stars [68]). Many mechanisms have been suggested for the origins of these CEMP-r/s stars (see the details in [69]), and the popular one is the mixed origin of the r- and s-process. This scenario suggests that the enriched r-process elements come from the molecular cloud where the star formed, while the enhanced s-process elements are from its massive companion in a binary system. The massive companion has evolved through the AGB stage, and it is a white dwarf now. The mechanism of their s-process enrichment is similar to the formation of the extrinsic Ba stars. The intermediate (i-) process (neutron number density of $10^{15-17} \cdot \mathrm{cm}^{-3}$ [70]) is another popular mechanism to explain the enrichment of CEMP-r/s stars, although its hosted sites are still in debate [71–75]. The i-process occurring in low-mass low-metallicity AGB stars can explain the abundances of CEMP-r/s stars successfully [76–78]. We noticed that BD+68°1027 has the highest $f_{\mathrm{odd,Ba}}$ value of 0.28 in our sample stars, which corresponds to a nearly equal contribution of the s- and r-process to its barium, i.e., 51% for the s-process and 49% for the r-process. In order to further investigate the r-process's contribution in BD+68°1027, we determined the abundances of Eu and Nd (see Table 5), that is [Eu/Fe] = +0.54 ± 0.19 dex (NLTE) and [Nd/Fe] = 0.60 ± 0.03 dex (LTE), which are consistent with those obtained by Kong et al. [24].

Table 5. The Nd and Eu abundances of our sample stars.

	BD+80°670	BD+68°1027	REJ 0702+129	HD 218356	HD 202109	HR 5692	HD 13611
$[\mathrm{Nd/Fe}]^{\mathrm{LTE}}$	–	0.60 ± 0.03	0.25 ± 0.06	0.73 ± 0.07	0.39 ± 0.04	0.21 ± 0.05	0.24 ± 0.04
$[\mathrm{Eu/Fe}]^{\mathrm{NLTE}}$	–	0.54 ± 0.19	0.30 ± 0.10	0.37 ± 0.10	0.30 ± 0.10	–	–

Figure 7 shows the abundance ratios of [Ba/Eu] and [Ba/Nd] versus $f_{\mathrm{odd,Ba}}$ for our sample stars, and BD+68°1027 is indicated as the filled square. According to Burris et al. [3],

the r-process is responsible for 97% of Eu, while 53% of Nd in the solar system; therefore, Eu is usually regarded as the representative element of the r-process. [Ba/Eu] is usually used as a probe of the r-process contribution, that is a lower [Ba/Eu] corresponds to a larger r-process contribution. From the upper panel of Figure 7, we can see that [Ba/Eu] shows good anti-correlation with $f_{\mathrm{odd,Ba}}$, which supports the fact that $f_{\mathrm{odd,Ba}}$ is a good probe for the r-process contribution. We note that [Ba/Nd] and $f_{\mathrm{odd,Ba}}$ are uncorrelated for most of our Ba stars, except BD+68°1027, which shows the lowest values of both [Ba/Eu] (+0.09 dex, the up-panel) and [Ba/Nd] (+0.03 dex (bottom-panel), while the highest $f_{\mathrm{odd,Ba}}$ value (0.28) among our Ba stars. This indicates that BD+68°1027 is a special one of our Ba samples, and it has a large r-process contribution to the barium abundance. In addition, we also note that the $f_{\mathrm{odd,Ba}}$ value (0.28 ± 0.11) of BD+68°1027 is almost equal to that (0.23 ± 0.12) of the CEMP-r/s star HE 0338-3945 [34]. Cui et al. [79] found that there are six Ba stars showing significant r-process features and defined them as r-rich Ba stars, of which the ratios of the s-process represented element La over Nd are almost lower than the solar one and similar to some of CEMP-r/s stars and all of the r-rich (r-I and r-II) stars. Therefore, we speculate that BD+68°1027 is also an r-rich Ba star, and it is likely to have similar origins to the CEMP-r/s stars.

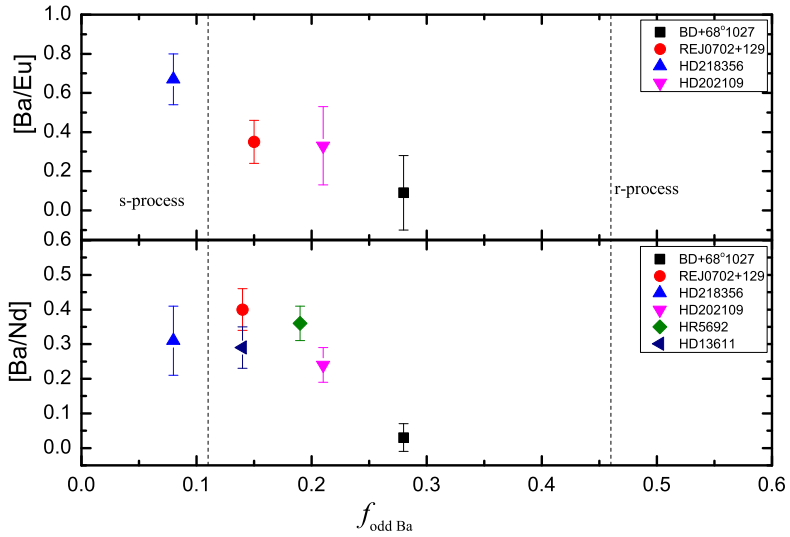

Figure 7. Top panel: the abundance ratio [Ba/Eu] vs. $f_{\mathrm{odd,Ba}}$; bottom panel: [Ba/Nd] vs. $f_{\mathrm{odd,Ba}}$. The two dotted lines represent $f_{\mathrm{odd,Ba}} = 0.11$ (the solar pure s-process) and $f_{\mathrm{odd,Ba}} = 0.46$ (the solar pure r-process) from Arlandini et al. [27].

5.5. Characters of $f_{\mathrm{odd,Ba}}$ in Ba Dwarfs and Ba Giants

To further study Ba stars, we show that the $f_{\mathrm{odd,Ba}}$ values vary with [Ba/Fe], [Ba/H], and [Fe/H] for the sample stars in Figure 8, and the results of r-II stars from Meng et al. [34] and Wenyuan et al. [35] are also included for comparison. From Figure 8, we can see that the $f_{\mathrm{odd,Ba}}$ values of r-II stars are significantly higher than those of Ba stars, which means that these two group of stars have different origins. Furthermore, there is no obvious difference of $f_{\mathrm{odd,Ba}}$ vs. [Ba/Fe], [Ba/H], and [Fe/H] between Ba dwarfs and giants, except the special Ba star HD 218356 and the possible metal-rich counterpart of the CEMP-r/s star BD+68°1027. In addition, for most of our Ba stars, their $f_{\mathrm{odd,Ba}}$ values are clustered around that of the solar one, which indicates that they do not experience additional r-process enrichment. In other words, like the Sun, the r-process contribution in these Ba stars can be naturally explained by the evolution of our Milky Way. Thus, we suggest that most of our Ba stars have a common enrichment history of their heavy elements, although their [Ba/Fe], [Ba/H], and [Fe/H] show a large dispersion.

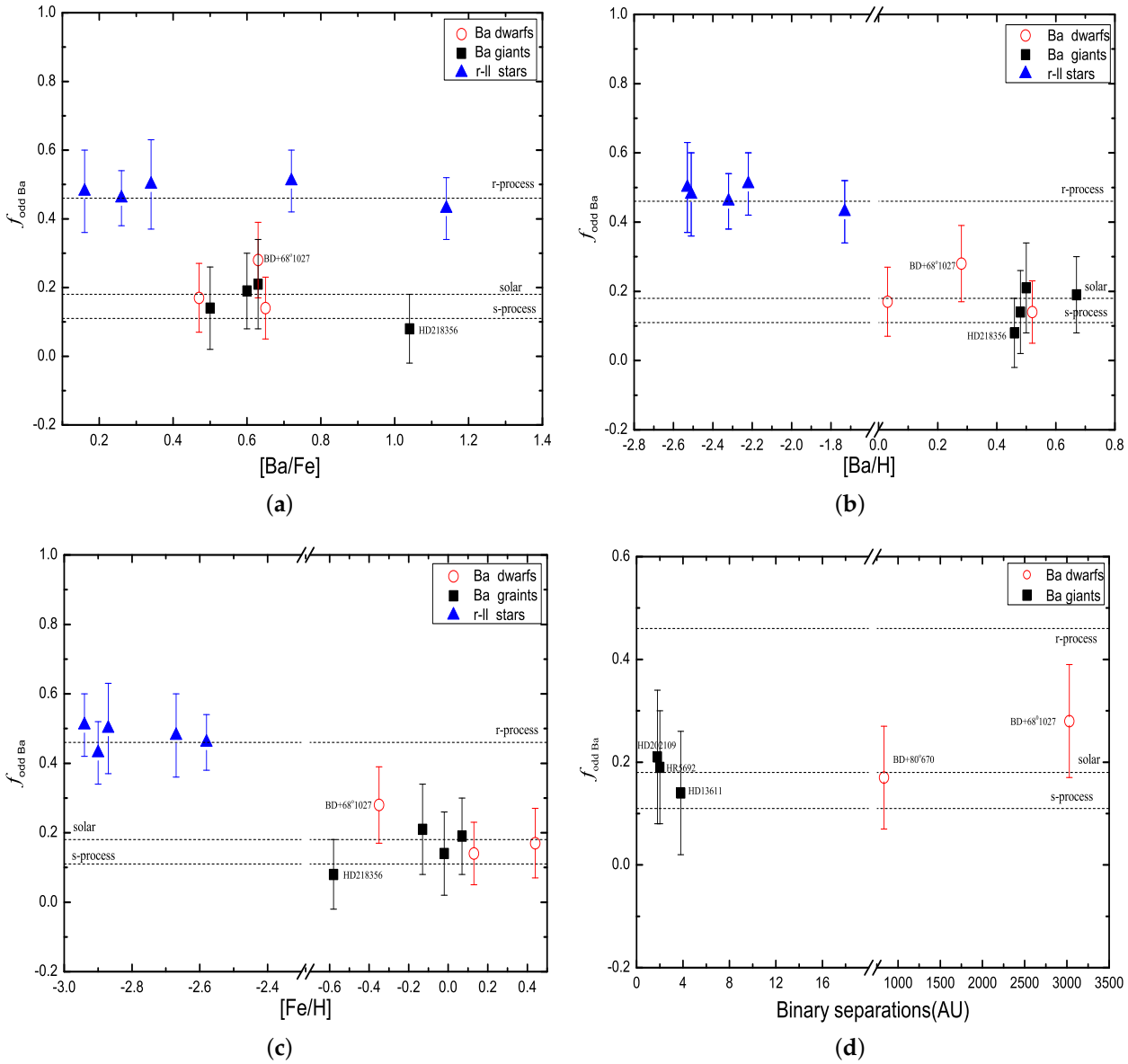

Figure 8. Fraction of the Ba odd isotopes versus [Ba/Fe] (**a**), [Ba/H] (**b**), [Fe/H] (**c**), and the orbital separation of binaries (**d**). The r-II stars (filled triangle) derived by Meng et al. [34] and Wenyuan et al. [35] are also included for comparison. There are three dotted horizontal lines: the upper line ($f_{\mathrm{odd,Ba}}$ = 0.46) for the pure r-process, the middle line ($f_{\mathrm{odd,Ba}}$ = 0.18) for the solar system, and the following line ($f_{\mathrm{odd,Ba}}$ = 0.11) for the pure s-process of the solar barium predicted by Arlandini et al. [27].

It has been generally accepted that the orbital separation of binary systems might play an important role in the efficiency of mass transfer and the level of s-process elements' enrichment in Ba stars [80]. The estimated semi-major axis (see Table 1) usually has been used to stand for the orbital separations. In our sample stars, BD+68°1027 has the maximum orbital separation value (3028 au), and the orbital separations for REJ 0702+129 and HD 218356 have not been determined. We plot the $f_{\mathrm{odd,Ba}}$ values against the orbital separations for the five sample stars in Figure 8d, and there is no obvious trend. Except the possible metal-rich CEMP-r/s counterpart BD+68°1027, the Ba dwarf BD+80°670 has almost the same $f_{\mathrm{odd,Ba}}$ value as those of other Ba giants in Figure 8d.

In addition, from Table 2, we can see that the mass of Ba dwarfs is smaller than that of Ba giants, which is consistent with the result of Kong et al. [24,37]. This result does not

support that the Ba dwarfs may be progenitors of Ba giants [11]. Of course, we are still not able to rule out the possibility of the evolution relations between Ba dwarfs and Ba giants due to our small Ba star samples; therefore, more Ba stars need to be investigated.

6. Conclusions

Based on the high resolution and high SNR spectra, we measured the $f_{\rm odd,Ba}$ values of seven Ba stars by fitting the Ba II resonance lines at 4554 Å following the method of Mashonkina and Zhao [33]. In order to obtain accurate results, we redetermined the stellar atmospheric parameters and Ba abundances taking NLTE effects into account. This is the first determination of the Ba odd isotopic fraction for Ba stars and will help us to understand the neutron capture nucleosynthesis for their heavy element enrichment:

- HD 218356 is likely to be a more evolved extrinsic Ba star at the stage of EAGB evolution based on its atmospheric parameters, the largest NLTE Ba abundance, and the lowest $f_{\rm odd,Ba}$ value in our Ba samples, whose massive companion should have the largest s-process efficiency in our Ba samples.
- BD+68°1027 have a large $f_{\rm odd,Ba}$ value of 0.28 ± 0.11, which is similar to the value 0.23 ± 0.12 of the CEMP-r/s star HE 0338-3945. Thus, we speculate that it is likely to be an r-rich Ba star, as suggested by Cui et al. [79], and to have similar origins to the CEMP-r/s stars.
- The $f_{\rm odd,Ba}$ values of the other five Ba stars spread around the solar value 0.18, which indicates that they do not experience additional r-process enrichment, and the evolution of the Milky Way can be responsible for the r-process contributions in these stars. Therefore, we suggest that these Ba stars have similar origins, that is the enrichment of heavy elements is due to the matter accretion occurring in a binary system.
- There is a good anti-correlation between the [Ba/Eu] and $f_{\rm odd,Ba}$ values for our Ba stars, and the effect of their orbital separations on $f_{\rm odd,Ba}$ is negligible. This indicates that $f_{\rm odd,Ba}$ could be a good probe for studying the neutron capture nucleosynthesis. Moreover, we note that the $f_{\rm odd,Ba}$ value predicted by the AGB models decreases with decreasing metallicities, which indicates that the $f_{\rm odd,Ba}$ value is also a direct tracer for the efficiency of the s-process nucleosynthesis.

Author Contributions: Conceptualization, W.C. and J.S.; data curation, F.W.; investigation, M.T. and X.Z.; writing—original draft, F.W.; writing—review and editing, W.C., J.S. and B.Z.; project administration, B.Z. All authors have read and agreed to the published version of the manuscript.

Funding: This work was supported by the National Key Basic R&D Program of China via 2019YFA0405500 and the National Natural Science Foundation of China (NSFC) under Grants 12173013, 12090040, 12090044, and 11833006. W.C. is supported by the 333 talents project 'A202010001' of Hebei Province, and W.C. and J.S. are also supported by the China Manned Space Project with No. CMS-CSST-2021-B05. This work was also supported by the Natural Science Foundation of Hebei Province under Grants A2021205006 and A2019110051 and by the project of Hebei provincial department of science and technology under Grant Number 226Z7604G.

Data Availability Statement: The data presented in this study are available upon request from the corresponding author.

Acknowledgments: Fang Wen expresses her appreciation to Xiaoming Kong for providing the spectral data and to Zhicun Liu for his technical help.

Conflicts of Interest: The authors declare no conflict of interest.

Notes

[1] $f_{\rm odd,Ba} = [N(^{135}{\rm Ba}) + N(^{137}{\rm Ba})]/N({\rm Ba})$, where N is the number density of Ba isotopes.

References

1. Bidelman, W.P.; Keenan, P.C. The Ba II Stars. *Astrophys. J.* **1951**, *114*, 473. [CrossRef]
2. Tomkin, J.; Lambert, D.L.; Edvardsson, B.; Gustafsson, B.; Nissen, P.E. HR 107—An F-type mild barium dwarf star. *Astron. Astrophys.* **1989**, *219*, L15–L18.
3. Burris, D.L.; Pilachowski, C.A.; Armroff, T.E.; Sneden, C.; Cowan, J.J.; Roe, H. Neutron-Capture Elements in the Early Galaxy: Insights from a Large Sample of Metal-poor Giants. *Astrophys. J.* **2000**, *544*, 302–319. [CrossRef]
4. Gallino, R. Evolution and Nucleosynthesis in Low-Mass Asymptotic Giant Branch Stars. II. Neutron Capture and the S-Process. *Astrophys. J.* **1998**, *497*, 388–403. [CrossRef]
5. Straniero, O.; Gallino, R.; Cristallo, S. s process in low-mass asymptotic giant branch stars. *Nucl. Phys. A* **2006**, *777*, 311–339. [CrossRef]
6. Woosley, S.E.; Wilson, J.R.; Mathews, G.J.; Hoffman, R.D.; Meyer, B.S. The r-Process and Neutrino-heated Supernova Ejecta. *Astrophys. J.* **1994**, *433*, 229. [CrossRef]
7. Rosswog, S.; Davies, M.B.; Thielemann, F.-K.; Piran, T. Merging neutron stars: Asymmetric systems. *Astron. Astrophys.* **2000**, *360*, 171–184.
8. Goriely, S.; Bauswein, A.; Just, O.; Pllumbi, E.; Janka, H.-T. Impact of weak interactions of free nucleons on the r-process in dynamical ejecta from neutron star mergers. *Mon. Not. R. Astron. Soc.* **2015**, *452*, 3894–3904. [CrossRef]
9. McClure, R.D.; Fletcher, J.M.; Nemec, J.M. The binary nature of the barium stars. *Astrophys. J.* **1980**, *238*, L35–L38. [CrossRef]
10. McClure, R.D. The binary nature of the barium stars. II. Velocities, binary frequency, and preliminary orbits. *Astrophys. J.* **1983**, *268*, 264–273. [CrossRef]
11. Böhm-Vitense, E.; Carpenter, K.; Robinson, R.; Ake, T.; Brown, J. Do All BA II Stars Have White Dwarf Companions? *Astrophys. J.* **2000**, *533*, 969–983. [CrossRef]
12. Bilíková, J.; Chu, Y.-H.; Gruendl, R. A.; Maddox, L.A. Hard X-ray Emission Associated with White Dwarfs. III. *Astron. J.* **2010**, *140*, 1433–1443. [CrossRef]
13. Gray, R.O.; McGahee, C.E.; Griffin, R.E.M.; Corbally, C.J. First Direct Evidence That Barium Dwarfs Have White Dwarf Companions. *Astron. J.* **2011**, *141*, 160. [CrossRef]
14. Bidelman, W.P. Objective-prism discoveries in the declination zone 0 to −20. *Astron. J.* **1981**, *86*, 553–556. doi: 10.1086/112913. [CrossRef]
15. Bidelman, W.P. Objective-prism discoveries in the Northern sky. I. *Astron. J.* **1983**, *88*, 1182–1186. [CrossRef]
16. Bidelman, W.P. Objective-prism discoveries in the northern sky. II. *Astron. J.* **1985**, *90*, 341–345. [CrossRef]
17. North, P.; Berthet, S.; Lanz, T. The nature of the F STR lambda 4077 stars. III. Spectroscopy of the barium dwarfs and other CP stars. *Astron. Astrophys.* **1994**, *281*, 775–796.
18. Porto de Mello, G.F.; da Silva, L. HR 6094: A Young, Solar-Type, Solar-Metallicity Barium Dwarf Star. *Astrophys. J.* **1997**, *476*, L89–L92. [CrossRef]
19. Pereira, C.B. Spectroscopic Verification of Barium Dwarf Candidates: The Analysis of HD 8270, HD 13551, and HD 22589. *Astron. J.* **2005**, *129*, 2469–2480. [CrossRef]
20. Gray, R.O.; Griffin, R.E.M. HD 26367: A Nearby, Newly Identified Barium Dwarf. *Astron. J.* **2007**, *134*, 96–101. [CrossRef]
21. Pompéia, L.; Allen, D.M. HD 11397 and HD 14282: Two new barium stars? *Astron. Astrophys.* **2008**, *488*, 723–729.:200809707. [CrossRef]
22. North, P.; Lanz, T. The nature of the F STR lambda 4077 stars. IV. Search for white dwarfs around barium dwarfs. *Astron. Astrophys.* **1991**, *251*, 489.
23. Edvardsson, B.; Andersen, J.; Gustafsson, B.; Lambert, D.L.; Nissen, P.E.; Tomkin, J. The chemical evolution of the galactic disk II. Observational data. *Astron. Astrophys. Suppl. Ser.* **1933**, *102*, 603.
24. Kong, X.M.; Bharat, K.Y.; Zhao, G.; Zhao, J.K.; Fang, X.S.; Shi, J.R.; Yan, H.L. Three new barium dwarfs with white dwarf companions: BD+68°1027, RE J0702+129 and BD+80°670. *Mon. Not. R. Astron. Soc.* **2018**, *474*, 2129. [CrossRef]
25. Cowley, C.R.; Frey, M. Hyperfine Structure in the Barium Resonance Line: Curves of Growth for Solar and r-Process Isotopic Mixtures. *Astrophys. J.* **1989**, *346*, 1030. [CrossRef]
26. Magain, P.; Zhao, G. Barium isotopes in the very metal-poor star HD 140283. *Astron. Astrophys.* **1993**, *268*, L27–L29.
27. Arlandini, C. Neutron Capture in Low-Mass Asymptotic Giant Branch Stars: Cross Sections and Abundance Signatures. *Astrophys. J.* **1999**, *525*, 886–900. [CrossRef]
28. Magain, P. Heavy elements in halo stars: The r/s-process controversy. *Astron. Astrophys.* **1995**, *297*, 686.
29. Lambert, D.L.; Allende Prieto, C. The isotopic mixture of barium in the metal-poor subgiant HD 140283. *Mon. Not. R. Astron. Soc.* **2002**, *335*, 325–334. [CrossRef]
30. Collet, R.; Asplund, M.; Nissen, P.E. The Barium Isotopic Abundance in the Metal-Poor Star HD140283. *Publ. Astron. Soc. Aust.* **2009**, *26*, 330–334. [CrossRef]
31. Gallagher, A.J.; Ryan, S.G.; García, P.A.E.; Aoki, W. The barium isotopic mixture for the metal-poor subgiant star HD 140283. *Astron. Astrophys.* **2010**, *523*, A24. [CrossRef]
32. Gallagher, A.J.; Ryan, S.G.; Hosford, A.; García, P.A.E.; Aoki, W.; Honda, S. The barium isotopic fractions in five metal-poor stars. *Astron. Astrophys.* **2012**, *538*, A118. [CrossRef]

33. Mashonkina, L.; Zhao, G. Barium even-to-odd isotope abundance ratios in thick disk and thin disk stars. *Astron. Astrophys.* **2006**, *456*, 313–321.:20054749. [CrossRef]
34. Meng, X.Y.; Cui, W.Y.; Shi, J.R.; Jiang, X.H.; Zhao, G.; Zhang, B.; Li, J. The odd isotope fractions of barium in CEMP-r/s star HE 0338-3945 and r-II star CS 31082-001. *Astron. Astrophys.* **2016**, *593*, A62. [CrossRef]
35. Wenyuan, C.; Xiaohua, J.; Jianrong, S.; Gang, Z.; Bo, Z. The Odd Isotope Fractions of Barium in the Strongly r-process-enhanced (r-II) Stars. *Astrophys. J.* **2018**, *854*, 131. [CrossRef]
36. Holberg, J.B.; Oswalt, T.D.; Sion, E.M.; Barstow, M.A.; Burleigh, M.R. Where are all the Sirius-like binary systems? *Mon. Not. R. Astron. Soc.* **2013**, *435*, 2077–2091. [CrossRef]
37. Kong, X.M. Chemical abundances of primary stars in the Sirius-like binary systems. *Mon. Not. R. Astron. Soc.* **2018**, *476*, 724–740. [CrossRef]
38. Gustafsson, B.; Edvardsson, B.; Eriksson, K.; Jørgensen, U.G.; Mizuno-Wiedner, M.; Plez, B. A New MARCS Grid. *Model. Stellar Atmos.* **2003**, *210*, A4.
39. Asplund, M. New Light on Stellar Abundance Analyses: Departures from LTE and Homogeneity. *Annu. Rev. Astron. Astrophys.* **2005**, *43*, 481–530. [CrossRef]
40. Sitnova, T. Systematic Non-LTE Study of the -2.6 < [Fe/H] < 0.2 F and G dwarfs in the Solar Neighborhood. I. Stellar Atmosphere Parameters. *Astrophys. J.* **2015**, *808*, 225. [CrossRef]
41. Grupp, F. MAFAGS-OS: New opacity sampling model atmospheres for A, F and G stars. I. The model and the solar flux. *Astron. Astrophys.* **2004**, *420*, 289–305.:20040971. [CrossRef]
42. Grupp, F.; Kurucz, R.L.; Tan, K. New extended atomic data in cool star model atmospheres. Using Kurucz's new iron data in MAFAGS-OS models. *Astron. Astrophys.* **2009**, *503*, 177–181. [CrossRef]
43. Kurucz, R.L. 2009 . Available online: http://kurucz.harvard.edu/atoms/2600/ (accessed on 12 July 2020).
44. Kurucz, R.L. 2009. Available online: http://kurucz.harvard.edu/atoms/2601/ (accessed on 12 July 2020).
45. Kurucz, R.L. 2009. Available online: http://kurucz.harvard.edu/atoms/2602/ (accessed on 12 July 2020).
46. Reetz, J.K. Sauerstoff in kühlen Sternen und die chemische Entwicklung der Galaxis. Ph.D. Thesis, Universität München, München, Germany, 1991.
47. Mashonkina, L.; Gehren, T.; Shi, J.-R.; Korn, A.J.; Grupp, F. A non-LTE study of neutral and singly-ionized iron line spectra in 1D models of the Sun and selected late-type stars. *Astron. Astrophys.* **2011**, *528*, A87. [CrossRef]
48. Bensby, T.; Feltzing, S.; Oey, M.S. Exploring the Milky Way stellar disk. A detailed elemental abundance study of 714 F and G dwarf stars in the solar neighbourhood. *Astron. Astrophys.* **2014**, *562*, a71. [CrossRef]
49. Butler, K.; Giddings, J. *Newsletter on the Analysis of Astronomical Spectra, No 9*; University of London: London, UK, 1985.
50. Gaia Collaboration. Gaia Data Release 3: Summary of the content and survey properties. *arXiv* **2022**, arXiv:2012.01533.
51. Lindegren, L. Gaia Early Data Release 3. Parallax bias versus magnitude, colour, and position. *Astron. Astrophys.* **2021**, *649*, A4. [CrossRef]
52. da Silva, L.; Girardi, L.; Pasquini, L.; Setiawan, J.; von der Luhe, O.; de Medeiros, J.R.; Hatzes, A.; Dollinger, M.P.; Weiss, A. Basic physical parameters of a selected sample of evolved stars. *Astron. Astrophys.* **2016**, *458*, 609–623.:20065105. [CrossRef]
53. Alonso, A.; Arribas, S.; Martínez-Roger, C. The effective temperature scale of giant stars (F0-K5). II. Empirical calibration of T_{eff} versus colours and [Fe/H]. *Astron. Astrophys. Suppl. Ser.* **1991**, *140*, 261–277.:1999521. [CrossRef]
54. Schlegel, D.J.; Finkbeiner, D.P.; Davis, M. Maps of Dust Infrared Emission for Use in Estimation of Reddening and Cosmic Microwave Background Radiation Foregrounds. *Astrophys. J.* **1998**, *500*, 525–553. [CrossRef]
55. Beers, T.C. Metal Abundances and Kinematics of Bright Metal-poor Giants Selected from the LSE Survey: Implications for the Metal-weak Thick Disk. *Astron. J.* **2002**, *124*, 931–948. [CrossRef]
56. Mashonkina, L.; Gehren, T.; Bikmaev, I. Barium abundances in cool dwarf stars as a constraint to s- and r-process nucleosynthesis. *Astron. Astrophys.* **1999**, *343*, 519–530.
57. Smith, V.V.; Lambert, D.L.; Nissen, P.E. Isotopic Lithium Abundances in Nine Halo Stars. *Astrophys. J.* **1998**, *506*, 405–423. [CrossRef]
58. Aoki, W.; Honda, S.; Beers, T.C.; Sneden, C. Measurement of the Europium Isotope Ratio for the Extremely Metal poor, r-Process-enhanced Star CS 31082-001. *Astrophys. J.* **2003**, *586*, 506. [CrossRef]
59. Cristallo, S. Evolution, Nucleosynthesis, and Yields of Low-mass Asymptotic Giant Branch Stars at Different Metallicities. II. The FRUITY Database. *Astrophys. J. Suppl. Ser.* **2011**, *197*, 17. [CrossRef]
60. Mathews, G.J.; Bazan, G.; Cowan, J.J. Evolution of Heavy-Element Abundances as a Constraint on Sites for Neutron-Capture Nucleosynthesis. *Astrophys. J.* **1992**, *391*, 719. [CrossRef]
61. Bubar, E.J.; King, J.R. Spectroscopic Abundances and Membership in the Wolf 630 Moving Group. *Astron. J.* **2010**, *140*, 293–318. [CrossRef]
62. Williams, M. First inverse kinematics study of the ^{22}Ne(p ,γ)^{23}Na reaction and its role in AGB star and classical nova nucleosynthesis. *Phys. Rev. C* **2020**, *102*, 035801-1. [CrossRef]
63. Dotter, A. MESA Isochrones and Stellar Tracks (MIST) 0: Methods for the Construction of Stellar Isochrones. *Astrophys. J. Suppl. Ser.* **2016**, *222*, 8. [CrossRef]
64. Choi, J.; Dotter, A.; Conroy, C.; Cantiello, M.; Paxton, B.; Johnson, B.D. Mesa Isochrones and Stellar Tracks (MIST). I. Solar-scaled Models. *Astrophys. J.* **2016**, *823*, 102. [CrossRef]

65. Paxton, B.; Bildsten, L.; Dotter, A.; Herwig, F.; Lesaffre, P.; Timmes, F. Modules for Experiments in Stellar Astrophysics (MESA). *Astrophys. J. Suppl. Ser.* **2011**, *192*, 3. [CrossRef]
66. Paxton, B. Modules for Experiments in Stellar Astrophysics (MESA): Planets, Oscillations, Rotation, and Massive Stars. *Astrophys. J. Suppl. Ser.* **2013**, *208*, 4. [CrossRef]
67. Paxton, B. Modules for Experiments in Stellar Astrophysics (MESA): Binaries, Pulsations, and Explosions. *Astrophys. J. Suppl. Ser.* **2015**, *220*, 15. [CrossRef]
68. Beers, T.C.; Christlieb, N. The Discovery and Analysis of Very Metal-Poor Stars in the Galaxy. *Annu. Rev. Astron. Astrophys.* **2005**, *43*, 531–580. [CrossRef]
69. Jonsell, K. The Hamburg/ESO R-process enhanced star survey (HERES). III. HE 0338-3945 and the formation of the r + s stars. *Astron. Astrophys.* **2006**, *451*, 651–670.:20054470. [CrossRef]
70. Cowan, J.J.; Rose, W.K. Production of 14C and neutrons in red giants. *Astrophys. J.* **1977**, *212*, 149. [CrossRef]
71. Fujimoto, M.Y.; Iben, I.; Hollowell, D. Helium Flashes and Hydrogen Mixing in Low-Mass Population III Stars. *Astrophys. J.* **1990**, *349*, 580. [CrossRef]
72. Fujimoto, M.Y.; Ikeda, Y.; Iben, I. The Origin of Extremely Metal-poor Carbon Stars and the Search for Population III. *Astrophys. J.* **2000**, *529*, L25–L28. [CrossRef]
73. Herwig, F. Convective-reactive Proton-^{12}C Combustion in Sakurai's Object (V4334 Sagittarii) and Implications for the Evolution and Yields from the First Generations of Stars. *Astrophys. J.* **2011**, *727*, 89. [CrossRef]
74. Dardelet, L. I process and CEMP-s+r stars. XIII Nuclei in the Cosmos (NIC XIII). *arXiv* **2014**, arXiv:1505.05500.
75. Denissenkov, P.A. I-process Nucleosynthesis and Mass Retention Efficiency in He-shell Flash Evolution of Rapidly Accreting White Dwarfs. *Astrophys. J.* **2017**, *834*, L10. [CrossRef]
76. Hampel, M.; Stancliffe, R.J.; Lugaro, M.; Meyer, B.S. The Intermediate Neutron-capture Process and Carbon-enhanced Metal-poor Stars. *Astrophys. J.* **2016**, *831*, 171. [CrossRef]
77. Goswami, P.P.; Rathour, R.S.; Goswami, A. Spectroscopic study of CEMP-(s & r/s) stars. Revisiting classification criteria and formation scenarios, highlighting i-process nucleosynthesis. *Astron. Astrophys.* **2021**, *649*, A49. [CrossRef]
78. Shejeelammal, J.; Goswami, A.; Shi, J. HCT/HESP study of two carbon stars from the LAMOST survey. *Mon. Not. R. Astron. Soc.* **2021**, *502*, 1008–1025. [CrossRef]
79. Cui, W.Y.; Zhang, B.; Shi, J.R.; Zhao, G.; Wang, W.J.; Niu, P. Possible discovery of the r-process characteristics in the abundances of metal-rich barium stars. *Astron. Astrophys.* **2014**, *566*, A16. [CrossRef]
80. Han, Z.; Eggleton, P.P.; Podsiadlowski, P.; Tout, C.A. The formation of barium and CH stars and related objects. *Mon. Not. R. Astron. Soc.* **1995**, *277*, 1443–1462. [CrossRef]